Superconductor Science and Technology

LETTER

In-field critical current performance of 4.0 μm thick film REBCO conductor with Hf addition at 4.2 K and fields up to 31.2 T

Letters

IOP Publishing

Superconductor Science and Technology

Supercond. Sci. Technol. **33** (2020) 07LT03 (8pp)

https://doi.org/10.1088/1361-6668/ab9541

Letter

In-field critical current performance of 4.0 μm thick film REBCO conductor with Hf addition at 4.2 K and fields up to 31.2 T

Goran Majkic[1], Rudra Pratap[1], Mahesh Paidpilli[1], Eduard Galstyan[1], Mehdi Kochat [1], Chirag Goel[1], Soumen Kar[2,1], Jan Jaroszynski[3], Dmytro Abraimov[3] and Venkat Selvamanickam[1]

[1] Department of Mechanical Engineering, Advanced Manufacturing Institute and Texas Center for Superconductivity, University of Houston, Houston, TX 77204 United States of America
[2] AMPeers LLC, Houston, TX 77059 United States of America
[3] Applied Superconductivity Center, National High Magnetic Field Laboratory, Florida State University, Tallahassee, Florida 32310 United States of America

E-mail: gmajkic@uh.edu

Received 5 March 2020, revised 30 April 2020
Accepted for publication 21 May 2020
Published 12 June 2020

Abstract

We present results on the in-field critical current (I_c) performance of 4.0 μm thick REBCO film with 15% Hf addition with fields up to 31.2 T and field orientations in the B||ab plane and B||c axis. Unlike the behavior at B||c, the critical current at B||ab is only very weakly dependent on field, decreasing from self-field to 31.2 T by only 22%, i.e. from the self-field value of ~7700 A/4 mm width to ~6300 and 5812 A/4 mm width at 14 and 30 T, respectively. These values are remarkably 3 and 5.7x higher than the corresponding critical currents at B||c. The in-field behavior of the present 15% Hf sample at field orientation B||c axis is nearly identical to the previously reported record values found in 4.3 and 4.6 μm thick 15% Zr samples in terms of critical current density. In contrast to the pinning force behavior in the B||c orientation, which saturates to a constant value of 1.7 TN m^{-3} above ~5–6 T, the pinning force in the B||ab orientation increases near-linearly, reaching a remarkable value of over 11.5 TN m^{-3} at 31.2 T. These results demonstrate the potential of thick REBCO conductors at 4.2 K for high field and energy density applications, in particular where the magnetic field is contained near the ab-plane.

Keywords: — High temperature superconductors, MOCVD, superconducting films, flux pinning, critical current

(Some figures may appear in colour only in the online journal)

1. Introduction

With continuous progress in the development of REBCO coated conductors, they have become increasingly attractive for low temperature (4.2–20 K) and intermediate to very high field applications, due to their high current density and the ability to operate at much higher fields compared to LTS conductors, opening possibilities for attaining very high magnetic fields and/or high magnetic energy density. Recently, an exciting fusion reactor project has been announced that

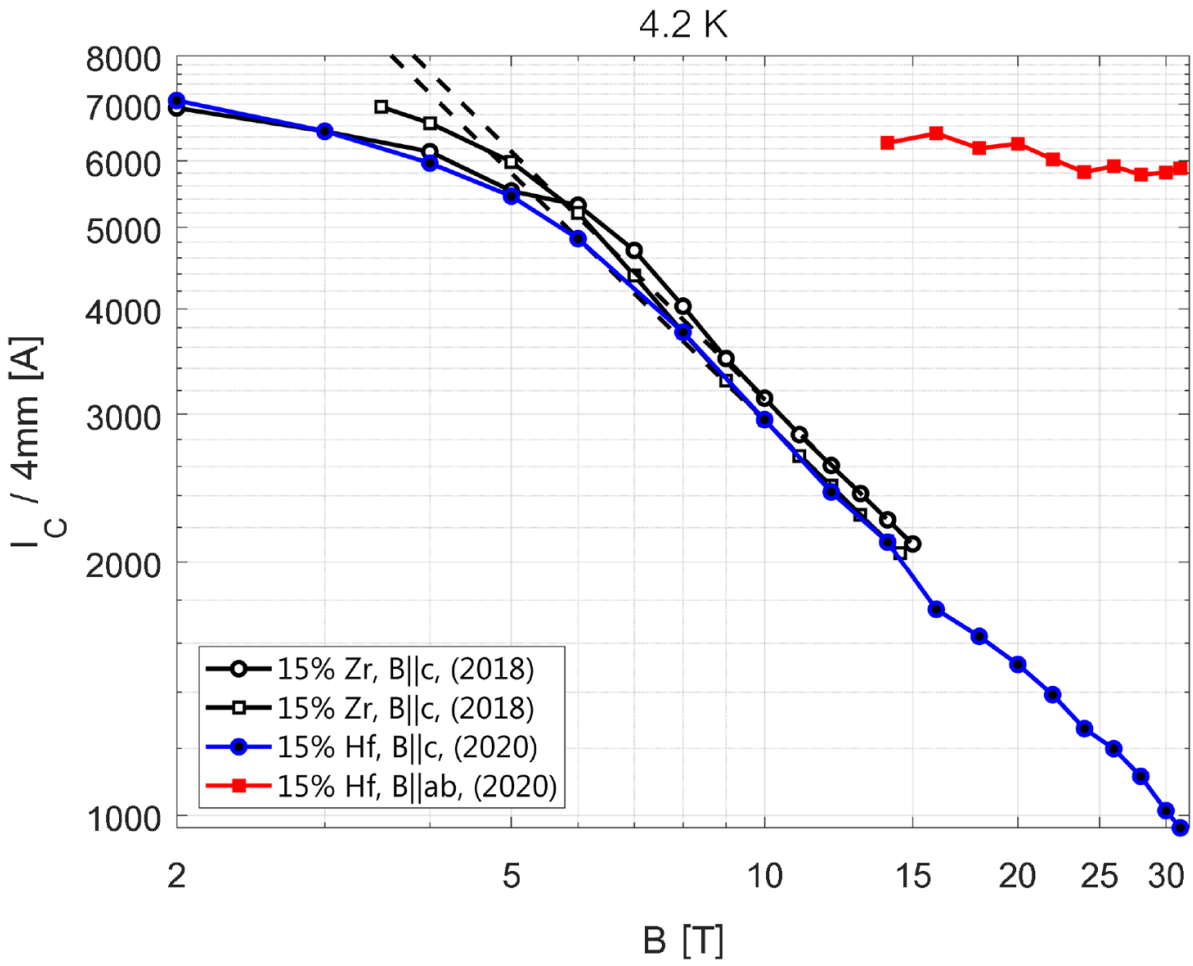

Figure 1. Critical current vs. magnetic field at 4.2 K for field orientations B||ab and B||c for the present 15% Hf-containing GdYBCO tape and I_c(B||c) of the previously reported 15% Zr containing GdYBCO tape [16]. The dashed lines are log-linear fit to the data above 9 T, with alpha value of 1.02.

would provide a net energy gain with a footprint of just a fraction of the ITER reactor, where the enabling technology is the REBCO conductor producing a field of 12 T (maximum field at conductor 21 T) at 20 K [1]. One can foresee the potential for significant further performance increase by increasing the critical current of the conductor and/or lowering the operating temperature towards 4.2 K. Other examples include the record 42.5 T magnet with a 13.5 T REBCO coil insert operating at 4.2 K, all-HTS magnet demonstrations and/or designs with fields of 25–32 T, a conceptual study of a steady state 100 T HTS magnet, various SMES devices operating at temperatures of 4.2–20 K, MRI coils and superconducting motors and generators [2–15].

Significant progress in understanding and overcoming obstacles to growing thick REBCO films with high current densities has been made in recent years [16–32]. Additionally, the understanding and control of the parameters influencing the effectiveness of artificial pinning centers (APC) in increasing in-field critical currents has significantly progressed from both fundamental and processing aspects [16–18, 20, 33–61]. Among the most studied systems are $BaZrO_3$ (BZO) and $BaHfO_3$ (BHO), with varying reports regarding whether either of the two systems has any clear advantage over the other.

We have recently reported the performance of 4+ μm thick REBCO films at 20–40 K and 4.2 K [16, 17]. The engineering current density (J_e) of the conductor at 4.2 K, 14 T at the 'worst' orientation B||c axis was measured at 5 kA mm^{-2} which constitutes an over five-fold increase over Nb_3Sn. However, the remaining unanswered question on the performance of these thick films is their performance at B||ab. For toroid-based designs (fusion tokamak, SMES), this field orientation is the most relevant, as the field is concentrated near the ab plane direction. In this letter, we report on both B||ab and B||c performance of a 4.0 μm thick film REBCO tape with 15% Hf addition at 4.2 K and fields up to 31.2 T. The main objectives are: 1.) to compare the optimized BHO sample to the performance of the previously reported optimized BZO sample at B||c where nanorods are effective pinning centers, and 2.) to compare the performance of the same tape in the B||ab plane relative to B||c.

2. Experimental

A (GdY)-Ba-Cu-O (GdY)BCO film containing 15% Hf was deposited using the advanced MOCVD (A-MOCVD) system

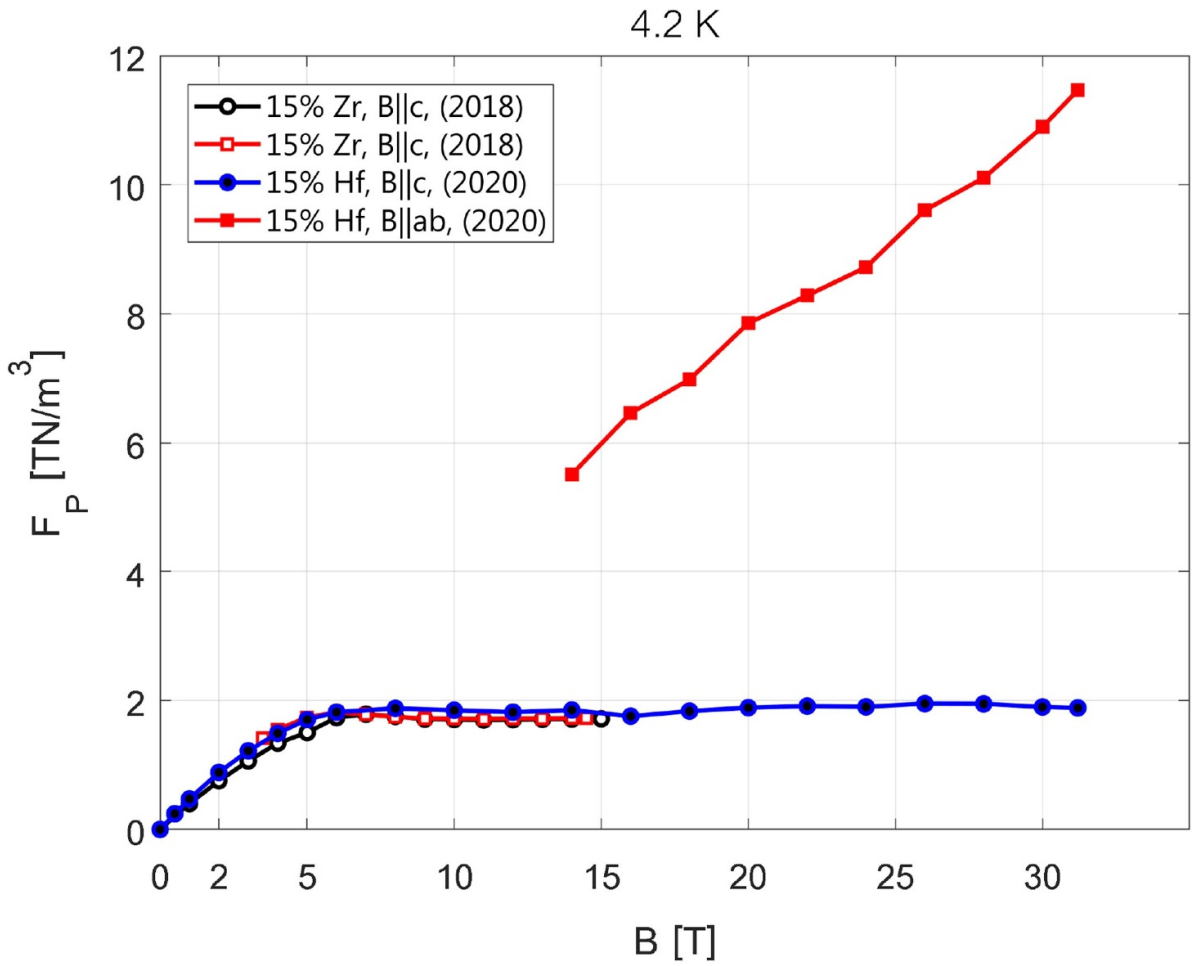

Figure 2. Pinning force vs. magnetic field at 4.2 K for field orientations B||ab and B||c for the present 15% Hf-containing GdYBCO tape and F_p(B||c) of the previously reported 15% Zr-containing GdYBCO tape [16].

[16–19], under deposition conditions described in [16]. The film was deposited on $LaMnO_3$ capped Hastelloy C276 tapes 12 mm wide over a deposition length of 30 cm. A microbridge with dimensions 80 × 500 μm was made using a focused ion beam (FIB) in order to enable measurement of very high currents at B||ab. In addition to the small size of the bridge that enabled measuring currents within the limits of the experimental setup, the FIB bridge also offers the advantage over etched bridges of the capability to sustain higher currents without delamination. The critical currents at B||ab and B||c orientations were measured on the same sample, as the FIB bridge survived measurements down to 0 T (self-field). The 2D-XRD measurements were performed in a new state-of-the-art facility at the University of Houston utilizing a microfocus source, Goebel mirror, 0.5 mm collimator and a high-resolution Vantec 500 detector. Transmission electron microscopy (TEM) was performed on a JEOL 2000FX microscope.

3. Results and discussion

Figure 1 shows the critical current at 4.2 K of the measured 15% Hf-containing GdYBCO sample at both orientations B||ab and B||c. For convenience, the previously-reported data on the 15% Zr samples at field orientation B||c are also superimposed on the graph. Two remarkable observations can be made from the data:

(a) The critical current at B||ab reaches 6300 A/4 mm-width at 14 T and 5812 A/4 mm-width at 30 T. These extraordinarily high values are 3 and 5.7x higher than the values obtained from the same sample at B||c with the same fields (2114 and 1013 A/4 mm, respectively).
(b) The critical current of the 15% Hf sample at B||c is nearly identical or practically identical to the previously reported 15% Zr samples, as well as the alpha value of 1.02 ($J \sim B^{-\alpha}$).

The corresponding critical current density values (J_c) at B||ab are 40.5 and 36.3 MA cm^{-2} at 14 and 30 T, respectively. In order to obtain an estimate of engineering current density, we use the same values as for the Zr sample [16] of 50 μm thick Hastelloy, 200 nm buffer, 40 μm Cu stabilizer and 3 μm thick silver, which leads to J_e values of 16.2 and 14.9 kA mm^{-2} at B||ab, 14 and 30 T, respectively. Compared to J_e ~1 kA mm^{-2} of Nb_3Sn at 15 T [62], the performance is higher by a factor of

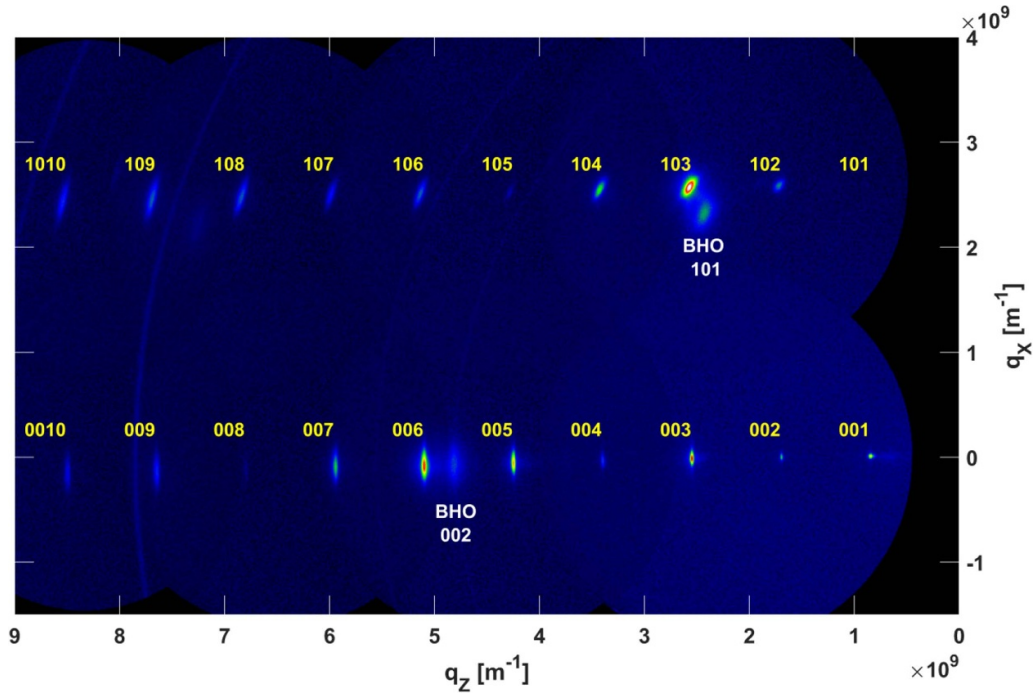

Figure 3. 2D-XRD diffraction pattern of the 4.0 μm thick GdYBCO film with 15% Hf addition. The pattern reveals sharp out of plane texture of GdYBCO, strong BZO (101) and (002) peaks, as well as absence of REO (004) and (222) peaks or any other secondary phase, including a-axis oriented GdYBCO grains.

over 16 times. The corresponding values for B||c are 5.4 and 2.6 kA mm^{-2} at 14 and 30 T.

Measurements of critical current of REBCO at 4.2 K, B||ab are relatively scarce (e.g. [55, 63],). The measurements on REBCO tapes from four commercial manufacturers at 12 and 14 T indicate about six-fold anisotropy of J_c between B||ab and B||c [63, 64]. From the measurements provided on a high J_e REBCO tape reported in [55, 62], we estimate J_e at B||ab and B||c of 3.42 and 0.53 kA mm^{-2} at 15 T and 2.72 and 0.33 kA mm^{-2} at 30 T, respectively. This constitutes J_c anisotropy of 6.5 at 15 T and 8.3 at 30 T. Regarding the J_e values at B||ab, the present data are higher by 4.7 and 5.5x at 15 and 30 T, respectively.

Figure 2 shows the pinning force for the same samples—the present 15% Hf-added GdYBCO at B||ab and B||c, as well as the previously reported 15% Zr-added GdYBCO at B||c. The pinning force in the B||c direction reaches a saturation point at ~5-6 T, identical for both Hf and Zr containing samples, after which it is constant up to 31.2 T at a level of 1.7 TN mm^{-2}. Remarkably, unlike the B||c direction, the pinning force in the B||ab direction near-linearly increases, reaching near 6 TN m^{-3} at 15 T and exceeding 10 TN m^{-3} at 30 T. The shape of the curve indicates no signs of saturation of F_p at fields immediately above 31.2 T, where it reaches 11.5 TN m^{-3}.

The magnitudes of the pinning force found in the present sample have strong implications in terms of opportunities that these results present for applications. For applications where field magnitude is of primary interest, the induced magnetic field B is directly proportional to I_c and the number of turns per unit length, n, $B \sim knI$, where k is a geometric constant dependent on the shape of the device. For a device operating at B||ab, this would constitute an 8–12 fold increase in peak magnitude for the same amount of tape, or alternatively, a 8–12 fold reduction of the amount of tape needed for the same field. However, for applications where magnetic energy density is of primary concern, $E \sim B^2 = knBI = knF_p$, therefore directly linearly proportional to the pinning force. This suggests that the magnetic energy density can be drastically increased by operating the device at 4.2 K and with very high fields, e.g. 30 T. On the other hand, for B||c, F_p is constant above 5–6 T, indicating that for energy density, there are no benefits to operating at fields higher than this saturation point. The calculated maximum compressive stress during the measurement at B||ab, 30 T was ~40 MPa, which the sample survived, as the measurements were completed in the sequence 15–31.2 T, followed by 31.2–0 T. The I_c values of repeated measurements between 15–31.2 T were near identical.

Figure 3 shows the 2D-XRD scan of the present Hf-containing sample, revealing sharp texture akin to that of the previously reported Zr sample [16], with no signs of unwanted secondary phases other than the $BaHfO_3$. The sample is purely c-axis oriented, with no trace of a-axis oriented grains, as also confirmed by scanning electron microscopy (SEM). One notable difference compared to the Zr-containing sample [16] is a complete lack of any of the rare earth oxide (RE_2O_3—REO) peaks in the present Hf sample, as can be seen by comparing the strong 004 and 222 REO peaks reported in [16] compared to the present sample. The fact that the Hf and Zr samples show near-identical B||c performance, despite a large difference in REO signal intensity, suggests that REO precipitates play no significant role in B||c pinning at 4.2 K. Further, by comparing

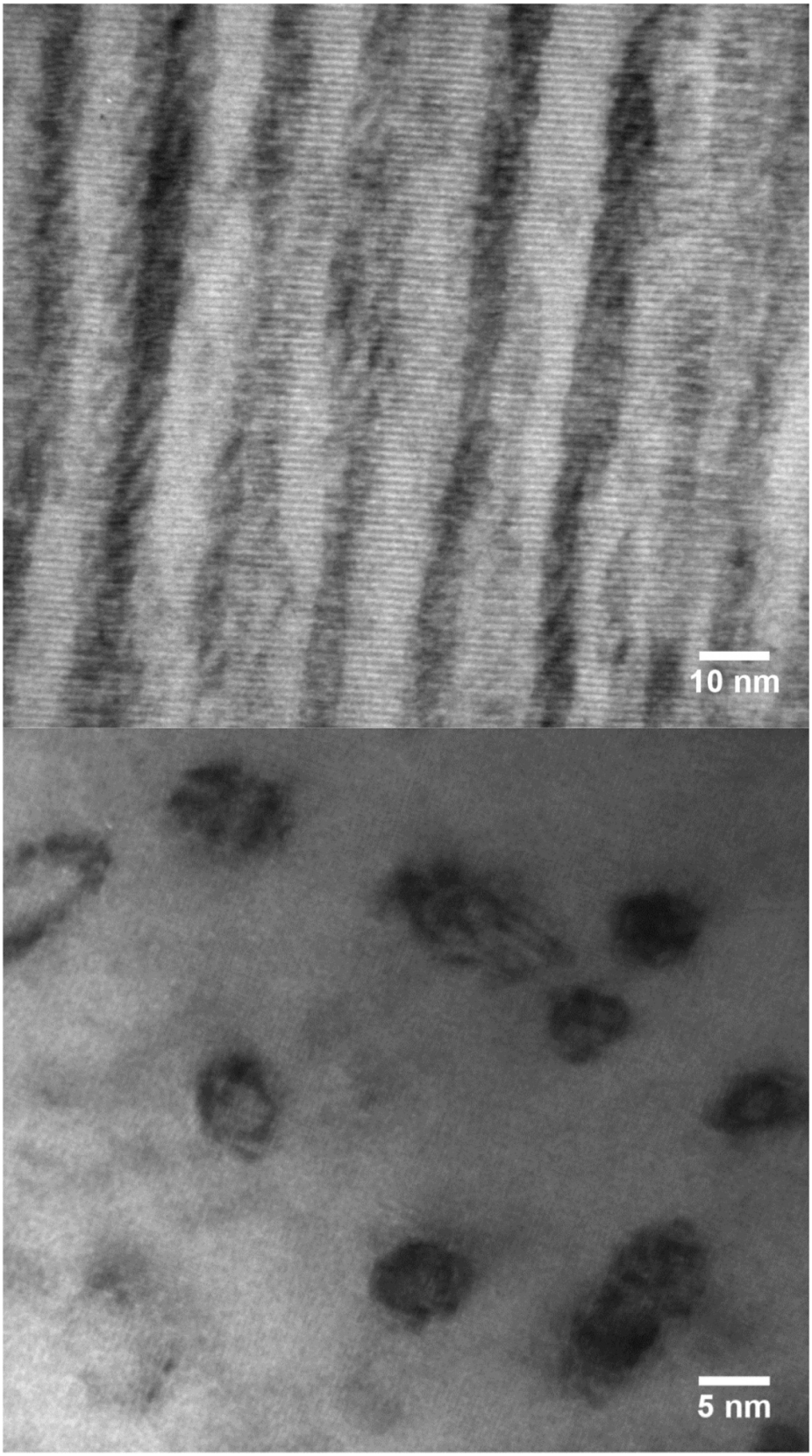

Figure 4. Cross-section and plane-view TEM micrographs of the 4.0 μm thick, 15% Hf-containing GdYBCO sample. The microstructure reveals continuous $BaHfO_3$ nanorods aligned along c-axis, and almost complete absence of RE_2O_3 precipitates. The average nanorod spacing and diameter are 18 and 5.4 nm, respectively.

the 101 BZO peaks, there are no obvious differences between the current Hf and the previously reported Zr samples.

Figure 4 shows a cross-section TEM micrograph of the present Hf sample. The average BHO nanorod diameter is 5.4 nm, which is larger than the 3.7 nm diameter found in the Zr sample [16]. On the other hand, the average spacing between nanorods has been estimated to be 18 nm, which is near-identical to the 19 nm average spacing found in the 15% Zr sample. The 18 nm spacing corresponds to a matching field of ∼6.4 T, which agrees well with the observed saturation field for the pinning force shown in figure 2. Regarding the REO precipitates, unlike the previously reported Zr sample and in accordance with the 2D-XRD results, there are no observable REO precipitates in the shown micrograph. We did observe some REO precipitates in this sample by TEM, but they have been found to be scarce compared to the TEM observations for the Zr sample [16].

4. Summary

An optimized REBCO sample with 15% mol. Hf addition and 4.0 μm thickness was produced using A-MOCVD and measured for I_c performance at 4.2 K both in B‖ab and B‖c orientations up to a maximum field of 31.2 T. The critical current at B‖ab reached remarkable values of 6300 and 5812 A/4 mm-width at 14 and 30 T, respectively, which are 3 and 5.7 times higher than the corresponding measured I_c(B‖c) values of 2114 and 1013 A/4 mm, respectively. The corresponding critical current density values are 40.5 and 36.3 MA cm^{-2} at 14 and 30 T, respectively. The critical current density of the present 15% Hf sample in the B‖c field orientation has been found to be near-identical to the values of the previously reported 4.3 and 4.6 μm thick REBCO films with 15% Zr addition [16]. The engineering current density performance at B‖ab, 15 T is over 16 times higher than that of Nb_3Sn. The pinning force at the B‖ab orientation exceeds 10 TN m^{-3} above 30 T, reaching 11.5 TN m^{-3} at 31.2 T.

Acknowledgments

This work was funded in part by the U.S. Department Energy Office of Science award DE-SC0016220. A portion of this work was performed at the National High Magnetic Field Laboratory, which is supported by National Science Foundation Cooperative Agreement No. DMR-1644779 and the State of Florida.

We acknowledge University of Houston Division of Research High Priority Area Research Large Equipment Grant I0503304 for establishing a state-of-the-art 2D-XRD facility used in this study.

ORCID iDs

Goran Majkic https://orcid.org/0000-0003-0168-0856
Eduard Galstyan https://orcid.org/0000-0003-1486-6449
Mehdi Kochat https://orcid.org/0000-0002-2928-0718
Soumen Kar https://orcid.org/0000-0001-5550-6859
Jan Jaroszynski https://orcid.org/0000-0003-3814-8468
Venkat Selvamanickam https://orcid.org/0000-0001-6618-9406

References

[1] Mumgaard B and Team S 2018 SPARC and the high-field path to commercial fusion energy 60th Annual Meeting of the APS Division of Plasma Physics
[2] Markiewicz W D, Weijers H W, Noyes P D, Trociewitz U P, Pickard K W, Sheppard W R, Jaroszynski J J, Xu A, Larbalestier D C and Hazelton D W, 2010 33.8 Tesla with a YBa2Cu3O7-x superconducting test coil *AIP Conf. Proc.* **1218** 225
[3] Breschi M, Cavallucci L, Ribani P L, Gavrilin A V and Weijers H W 2016 Analysis of quench in the NHMFL REBCO prototype coils for the 32T Magnet Project *Supercond. Sci. Technol.* **29**
[4] Markiewicz W D *et al* 2012 Design of a superconducting 32 T magnet with REBCO high field coils *IEEE Trans. Appl. Supercond.* **22**
[5] Weijers H W *et al* 2014 Progress in the Development of a Superconducting 32 T magnet with REBCO high field coils *IEEE Trans. Appl. Supercond.* **24**
[6] Bruzzone P, Wesche R, Uglietti D and Bykovsky N 2017 High temperature superconductors for fusion at the swiss plasma center *Nucl. Fusion* **57**
[7] Fietz W H, Barth C, Drotziger S, Goldacker W, Heller R, Schlachter S I and Weiss K P 2013 Prospects of high temperature superconductors for fusion magnets and power applications *Fusion Eng. Des.* **88** 440–5
[8] Gupta R *et al* 2015 Hybrid high-field cosine-theta accelerator magnet R&D with second-generation HTS *IEEE Trans. Appl. Supercond.* **25**
[9] Miyazaki H *et al* 2016 Design of a conduction-cooled 9.4T REBCO magnet for whole-body MRI systems *Supercond. Sci. Technol.* **29**
[10] Yokoyama S *et al* 2017 Research and development of the high stable magnetic field ReBCO coil system fundamental technology for MRI *IEEE Trans. Appl. Supercond.* **27**
[11] Yoon S, Kim J, Lee H, Hahn S and Moon S H 2016 26T 35mm all-GdBa2Cu3O7-x multi-width no-insulation superconducting magnet *Supercond. Sci. Technol.* **29**
[12] Kim K, Bhattarai K R, Jang J Y, Hwang Y J, Yoon S, Lee S and Hahn S 2017 Design and performance estimation of a 35 T 40 mm no-insulation all-REBCO user magnet *Supercond. Sci. Technol.* **30**
[13] Iwasa Y and Hahn S 2013 First-cut design of an all-superconducting 100-T direct current magnet *Appl. Phys. Lett.* **103**
[14] Lloberas J, Sumper A, Sanmarti M and Granados X 2014 A review of high temperature superconductors for offshore wind power synchronous generators *Renew. Sustain. Energy Rev.* **38** 404–14
[15] Moon H, Kim Y C, Park H J, Yu I K and Park M 2016 An introduction to the design and fabrication progress of a megawatt class 2G HTS motor for the ship propulsion application *Supercond. Sci. Technol.* **29**
[16] Majkic G, Pratap R, Xu A X, Galstyan E, Higley H C, Prestemon S O, Wang X R, Abraimov D, Jaroszynski J and Selvamanickam V 2018 Engineering current density over 5kAmm(−2) at 4.2K, 14T in thick film REBCO tapes *Supercond. Sci. Technol.* **31**
[17] Majkic G, Pratap R, Xu A X, Galstyan E and Selvamanickam V 2018 Over 15 MA/cm(2) of critical current density in 4.8 mu m thick, Zr-doped (Gd,Y)Ba2Cu3Ox superconductor at 30 K, 3T *Sci. Rep.* **8**

[18] Majkic G, Pratap R, Galstyan E, Xu A X, Zhang Y and Selvamanickam V 2017 Engineering of nanorods for superior in field performance of 2G-HTS conductor utilizing advanced MOCVD reactor *IEEE Trans. Appl. Supercond.* **27**

[19] Majkic G, Galstyan E and Selvamanickam V 2015 High performance 2G-HTS wire using a novel MOCVD System *IEEE Trans. Appl. Supercond.* **25**

[20] Majkic G 2020 Progress in thick film 2G-HTS development *Superconductivity*, ed P Mele, K Prassides, C Tarantini, A Palau, P Badica, A K Jha and T Endo (Berlin: Springer) pp 73–131

[21] Ha H S, Lee J H, Ko R K, Kim H S, Kim H K, Moon S H, Park C, Youm D J and Oh S S 2010 Thick SmBCO/IBAD-MgO coated conductor for high current carrying power applications *IEEE Trans. Appl. Supercond.* **20** 1545–8

[22] Rostila L, Lehtonen J and Mikkonen R 2007 Self-field reduces critical current density in thick YBCO layers *Physica* C **451** 66–70

[23] Igarashi M *et al* 2010 High-speed deposition of RE123 film with large current capacity by hot-wall type PLD system *Physica* C **470** 1230–3

[24] Durrschnabel M, Aabdin Z, Bauer M, Semerad R, Prusseit W and Eibl O 2012 DyBa2Cu3O7-x superconducting coated conductors with critical currents exceeding 1000 A cm(−1) *Supercond. Sci. Technol.* **25**

[25] Kim G, Jin H J, Jo W, Nam D H, Cheong H, Kim H S, Oh S S, Ko R K, Jo Y S and Ha D W 2015 Ultra-large current transport in thick SmBa2Cu3O7-x films grown by reactive co-evaporation *Physica* C **513** 29–34

[26] Kim H S, Oh S S, Ha H S, Youm D, Moon S H, Kim J H, Dou S X, Heo Y U, Wee S H and Goyal A 2015 Ultra-high performance, high-temperature superconducting wires via cost-effective, scalable, co-evaporation process *Sci. Rep.* **4** 4474

[27] Liu L, Li Y, Wu X, Xiao G and Xu D 2015 Development of long REBCO coated conductors by PLD-REBCO/Sputter-CeO2/IBAD-MgO at SJTU and SSTC *IEEE Trans. Appl. Supercond.* **25**

[28] Liu L F, Li Y Y, Xiao G N and Wu X 2015 Fabrication of thick REBCO-coated conductors with high performance on metal tapes by pulsed laser deposition process *J. Supercond. Novel Magnet.* **28** 403–6

[29] Fujita S *et al* 2018 Development of long-length BMO-doped REBCO coated conductors by hot-wall PLD process *IEEE Trans. Appl. Supercond.* **28**

[30] Iijima Y *et al* 2017 BMO-doped REBCO-coated conductors for uniform in-field I-c by hot-wall PLD process using IBAD template *IEEE Trans. Appl. Supercond.* **27**

[31] Sieger M, Pahlke P, Lao M, Meledin A, Eisterer M, Van Tendeloo G, Schultz L, Nielsch K and Huhne R 2018 Thick secondary phase pinning-enhanced YBCO films on technical templates *IEEE Trans. Appl. Supercond.* **28**

[32] Selvamanickam V *et al* 2009 High performance 2G wires: from R&D to pilot-scale manufacturing *IEEE Trans. Appl. Supercond.* **19** 3225–30

[33] Macmanus-Driscoll J L, Foltyn S R, Jia Q X, Wang H, Serquis A, Civale L, Maiorov B, Hawley M E, Maley M P and Peterson D E 2004 Strongly enhanced current densities in superconducting coated conductors of YBa2Cu3O7−x+BaZrO3 *Nat. Mater.* **3** 439–43

[34] Matsumoto K and Mele P 2010 Artificial pinning center technology to enhance vortex pinning in YBCO coated conductors *Supercond. Sci. Technol.* **23**

[35] Yamada Y *et al* 2005 Epitaxial nanostructure and defects effective for pinning in Y(RE)Ba2Cu3O7-x coated conductors *Appl. Phys. Lett.* **87**

[36] Tobita H, Notoh K, Higashikawa K, Inoue M, Kiss T, Kato T, Hirayama T, Yoshizumi M, Izumi T and Shiohara Y 2012 Fabrication of BaHfO3 doped Gd1Ba2Cu3O7-delta coated conductors with the high I-c of 85 A/cm-w under 3 T at liquid nitrogen temperature (77 K) *Supercond. Sci. Technol.* **25**

[37] Xu A X *et al* 2015 Broad temperature pinning study of 15 mol.% Zr-Added (Gd, Y)-Ba-Cu-O MOCVD coated conductors *IEEE Trans. Appl. Supercond.* **25** 5

[38] Lei C H, Galstyan E, Chen Y M, Shi T, Liu Y H, Khatri N, Liu J F, Xiong X M, Majkic G and Selvamanickam V 2013 The structural evolution of (Gd, Y)Ba2Cu3Ox tapes With Zr addition made by metal organic chemical vapor deposition *IEEE Trans. Appl. Supercond.* **23** 4

[39] Majkic G, Yao Y, Liu J G, Liu Y H, Khatri N D, Shi T, Chen Y M, Galstyan E, Lei C H and Selvamanickam V 2013 Effect of high BZO dopant levels on performance of 2G-HTS MOCVD wire at intermediate and low temperatures *IEEE Trans. Appl. Supercond.* **23** 5

[40] Chen Y, Selvamanickam V, Zhang Y, Zuev Y, Cantoni C, Specht E, Paranthaman M P, Aytug T, Goyal A and Lee D 2009 Enhanced flux pinning by BaZrO 3 and (Gd, Y) 2 O 3 nanostructures in metal organic chemical vapor deposited GdYBCO high temperature superconductor tapes *Appl. Phys. Lett.* **94** 062513–062513-3

[41] Miura M, Maiorov B, Sato M, Kanai M, Kato T, Izumi T, Awaji S, Mele P, Kiuchi M and Matsushita T 2017 Tuning nanoparticle size for enhanced functionality in perovskite thin films deposited by metal organic deposition *Npg Asia Mater.* **9**

[42] Mele P *et al* 2015 High pinning performance of YBa2Cu3O7-x films added with Y2O3 nanoparticulate defects *Supercond. Sci. Technol.* **28** 9

[43] Mele P, Matsumoto K, Horide T, Ichinose A, Mukaida M, Yoshida Y and Horii S 2007 Insertion of nanoparticulate artificial pinning centres in YBa2Cu3O7-x films by laser ablation of a Y2O3- surface modified target *Supercond. Sci. Technol.* **20** 616–20

[44] Gharahcheshmeh M H, Majkic G, Galstyan E, Xu A, Zhang Y, Li X F and Selvamanickam V 2018 Control of in-field performance of 25 mol.% Zr-added REBCO superconductor tapes *Physica* C **553** 26–32

[45] Gharahcheshmeh M H, Galstyan E, Xu A, Kukunuru J, Katta R, Zhang Y, Majkic G, Li X F and Selvamanickam V 2017 Superconducting transition width (Delta T-c) characteristics of 25mol% Zr-added (Gd, Y) Ba2Cu3O7-delta superconductor tapes with high in-field critical current density at 30K *Supercond. Sci. Technol.* **30**

[46] Xu A *et al* 2017 J(e)(4.2 K, 31.2 T) beyond 1 kA/mm(2) of a similar to 3.2 mu m thick, 20 mol% Zr-added MOCVD REBCO coated conductor *Sci. Rep.* **7** 6853

[47] Miura S, Yoshida Y, Ichino Y, Xu Q, Matsumoto K, Ichinose A and Awaji S 2016 Improvement in J(c) performance below liquid nitrogen temperature for SmBa2Cu3Oy superconducting films with BaHfO3 nano-rods controlled by low-temperature growth *Apl. Mater.* **4**

[48] Selvamanickam V, Mallick R, Tao X, Yao Y, Gharahcheshmeh M H, Xu A, Zhang Y, Galstyan E and Majkic G 2016 Improved flux pinning by prefabricated SnO2 nanowires embedded in epitaxial YBa2Cu3Ox superconducting thin film tapes *Supercond. Sci. Technol.* **29**

[49] Galstyan E, Gharahcheshmeh M H, Delgado L, Xu A X, Majkic G and Selvamanickam V 2015 Microstructure characteristics of high lift factor MOCVD REBCO coated conductors with high Zr content *IEEE Trans. Appl. Supercond.* **25** 5

[50] Selvamanickam V, Gharahcheshmeh M H, Xu A, Zhang Y and Galstyan E 2015 Critical current density above

15MAcm(−2) at 30K, 3T in 2.2 mu m thick heavily-doped (Gd,Y) Ba2Cu3Ox superconductor tapes *Supercond. Sci. Technol.* **28** 072002
[51] Selvamanickam V, Gharahcheshmeh M H, Xu A, Galstyan E, Delgado L and Cantoni C 2015 High critical currents in heavily doped (Gd,Y)Ba2Cu3Ox superconductor tapes *Appl. Phys. Lett.* **106** 5
[52] Xu A, Delgado L, Gharahcheshmeh M H, Khatri N, Liu Y and Selvamanickam V 2015 Strong correlation between J(c)(T, H parallel to c) and J(c)(77 K, 3 T parallel to c) in Zr-added (Gd, Y)BaCuO coated conductors at temperatures from 77 down to 20 K and fields up to 9 T *Supercond. Sci. Technol.* **28** 6
[53] Selvamanickam V, Xu A, Liu Y, Khatri N D, Lei C, Chen Y, Galstyan E and Majkic G 2014 Correlation between in-field critical currents in Zr-added (Gd, Y)Ba2Cu3Ox superconducting tapes at 30 and 77 K *Supercond. Sci. Technol.* **27**
[54] Xu A, Delgado L, Khatri N, Liu Y, Selvamanickam V, Abraimov D, Jaroszynski J, Kametani F and Larbalestier D C 2014 Strongly enhanced vortex pinning from 4 to 77 K in magnetic fields up to 31 T in 15 mol.% Zr-added (Gd, Y)-Ba-Cu-O superconducting tapes *Apl. Mater.* **2** 8
[55] Braccini V *et al* 2011 Properties of recent IBAD-MOCVD coated conductors relevant to their high field, low temperature magnet use *Supercond. Sci. Technol.* **24**
[56] Takahashi K, Kobayashi H, Yamada Y, Ibi A, Fukushima H, Konishi M, Miyata S, Shiohara Y, Kato T and Hirayama T 2006 Investigation of thick PLD-GdBCO and ZrO2 doped GdBCO coated conductors with high critical current on PLD-CeO2 capped IBAD-GZO substrate tapes *Supercond. Sci. Technol.* **19** 924
[57] Shi J J and Wu J Z 2015 Influence of the lattice strain decay on the diameter of self assembled secondary phase nanorod array in epitaxial films *J. Phys. D: Appl. Phys.* **118**
[58] Wu J Z, Shi J J, Baca J F, Emergo R, Haugan T J, Maiorov B and Holesinger T 2014 The effect of lattice strain on the diameter of BaZrO3 nanorods in epitaxial YBa2Cu3O7-delta films *Supercond. Sci. Technol.* **27**
[59] Shi J J and Wu J Z 2012 Micromechanical model for self-organized secondary phase oxide nanorod arrays in epitaxial YBa2Cu3O7-delta films *Philos. Mag.* **92** 2911–22
[60] Wang X, Baca F J, Emergo R L S, Wu J Z, Haugan T J and Barnes P N 2010 Eliminating thickness dependence of critical current density in YBa2Cu3O7-x films with aligned BaZrO3 nanorods *J. Phys. D: Appl. Phys.* **108**
[61] Gharahcheshmeh M H, Galstyan E, Kukunuru J, Katta R, Majkic G, Li X F and Selvamanickam V 2017 MOCVD of heavily-doped 25 mol.% Zr-added (Gd, Y) Ba2Cu3O7-delta coated conductors *IEEE Trans. Appl. Supercond.* **27**
[62] Lee P Comparisons of critical and engineering current densities for superconductors available in long lengths (avaliable at: https://nationalmaglab.org/magnet-development/applied-superconductivity-center/plots
[63] Uglietti D, Kitaguchi H, Choi S and Kiyoshi T 2009 Angular dependence of critical current in coated conductors at 4.2 K and magnet design *IEEE Trans. Appl. Supercond.* **19** 2909–12
[64] Uglietti D 2019 A review of commercial high temperature superconducting materials for large magnets: from wires and tapes to cables and conductors *Supercond. Sci. Technol.* **32**